FINITE ELEMENT ANALYSIS OF POWDERED MAGNET SINTER-FORGING PROCESSES CONSIDERING DEFORMABLE BODY CONTACT

S. H. Kim, H. W. Lee, H. Huh, C. H. Lee † and K. S. Ahn ††

Dept. of Mechanical Engineering
Korea Advanced Institute of Science and Technology
373-1 Science Town, Taejon, 305-701, Korea

† Dept. of Mechanical Engineering, Northwestern University
2145 Sheridan Rd., Evanston IL, 60208 USA

†† Research & Development Center, Mando Machinery Corporation,
95, Dukso-ri, Wabu-eub, Namyangju-city, Kyongki-do, 472-900, Korea

Abstract

Tube Process (TP) is a process to produce permanent magnets using a deformable tube for densification of magnet powder. This process claims that it can accomplish both densification and anisotropication in one step forming. This process is distinguished from other processes since it uses a deformable copper tube for densification of magnet powder. In this paper, simulation has been carried out for the Tube Process in a closed die considering the compressibility of powdered material, arbitrary curved shape and deformable body contact between Nd-Fe-B magnet powder and a copper tube. Results show that the finite element analysis of the Tube Process plays an important role in the stage of preform design.

Key Words : Tube Process; Powdered Magnet; Deformable body contact

1. Introduction

Since permanent magnets of Nd-Fe-B group were produced on a commercial scale in 1984, they have kept a key post in the permanent magnet market and are expected to continue steady and remarkable growth. The magnets are currently used in electric machines, high energy motors, generators, sensors and so on. The Nd-Fe-B magnet is manufactured by the sintering process, the GM Process (Rapid Solidification and Hot Forming Process) or the HDDR Process (Hydrogenation Decomposition Desorption Recombination Process). All processes are protected by patents against its application without license. In order to overcome this obstacle of the patents, Tube Process (TP) was developed and patented by Mando Machinery Corporation in Korea. TP is one of the processes to produce permanent magnets by sinter-forging in the closed die with the use of deformable tube. Advantage claimed for this process is that it can accomplish both densification and anisotropication in one step forming. This process is distinguished from other processes since it uses deformable copper tube for densification of magnet powder. TP has, however, difficulties in manufacturing permanent magnets from Nd-Fe-B green powder because of folding from large height reduction and localized densification. Therefore, a through study on preform and near net shape manufacturing is necessary for commercial scale production [9].

Numerous studies have been made both theoretically and numerically for the forming of the powdered metals[1-

8]. These researches were, however, confined to a single powder material. Compared to previous researches, TP should be carried out with a deformable tube and magnet powder. Preform design for TP is not easy due to the complexity of the process. The design cost and time can be remarkably reduced with the aid of the finite element analysis.

In this paper, a rigid-plastic finite element code has been developed to consider the compressibility of the powder material and deformable body contact with 8-node hexahedral isoparametric elements. The analysis deals with curved die and punch surfaces since commercial powdered magnet has the shape of circular arc. For the treatment of punch and dies, the code uses arbitrary curved surfaces by finite element patch. The code adopts a Lagrange multiplier method for contact treatment. There are two types of contact: one is contact between die surfaces and material surfaces; and the other is contact between magnet powder and a tube. The simulation has been carried out for a full TP in a closed die considering the compressibility of material, arbitrary curved shape and two contact types. TP for flat-type square magnets is simulated with simple finite element meshes to evaluate the validity of the present code and arc-shaped magnets for EHPS (Electro-Hydraulic Power Steering) system is simulated for preform design. In order to achieve the net-shape manufacturing by reducing the flash and folding of the tube, the optimum preform of slanted shape is chosen with the proper initial dimension. Results show that the finite element analysis of TP is indispensable in the stage of preform design.

2. Theoretical derivation

2.1 Constitutive equations

An yield function for powder material (P/M) can be expressed by the second invariant of the stress deviation tensor J_2' and the first invariant of the stress tensor J_1 as [10]:

$$f(\sigma_{ij}) = A\,J_2' + B\,J_1^2 = \eta\,Y_o^2 = \tilde{\sigma}^2 \tag{1}$$

where Y_o is the uniaxial yield stress of a matrix material, $\tilde{\sigma}$ is the flow stress of P/M and A , B , η are the function of the relative density. For the uniaxial stress state, the constitutive equations can be expressed as [10]:

$$\dot{\varepsilon}_{ij} = \frac{\tilde{\dot{\varepsilon}}}{\tilde{\sigma}}\left\{\frac{A}{2}\sigma_{ij} + \frac{3}{2}(2-A)\sigma_m\delta_{ij}\right\} \tag{2}$$

$$\sigma_{ij} = \frac{\tilde{\sigma}}{\tilde{\dot{\varepsilon}}}\left\{\frac{2}{A}\dot{\varepsilon}_{ij} + \frac{3(2-A)}{2A(3-A)}\dot{\varepsilon}_v\delta_{ij}\right\} \tag{3}$$

where $\dot{\varepsilon}_{ij}$ is the strain rate tensor, σ_{ij} is the stress tensor, $\tilde{\dot{\varepsilon}}$ is the effective strain rate of P/M, σ_m is the mean stress and $\dot{\varepsilon}_v$ is the volumetric strain rate. For the uniaxial stress state, the effective strain rate and volumetric strain rate can be expressed as follows:

$$\tilde{\dot{\varepsilon}}^2 = \frac{2}{A}\dot{\varepsilon}_{ij}'\dot{\varepsilon}_{ij}' + \frac{\dot{\varepsilon}_v^{\,2}}{3(3-A)}\delta_{ij} \tag{4}$$

$$\dot{\varepsilon}_v = -\frac{d\rho}{\rho} = \frac{dV}{V} = 3(3-A)\sigma_m\frac{\tilde{\dot{\varepsilon}}}{\tilde{\sigma}} \tag{5}$$

where V is the volume of P/M and ρ is the relative density.

2.2 Finite element formulation

The plastic potential energy for P/M can be defined by a functional as follows[11]:

$$\delta\tilde{\Phi} = \int_{\Omega}\tilde{\sigma}\,\delta\tilde{\dot{\varepsilon}}\,d\Omega - \int_{\Gamma_f} f_i\,\delta v_i\,d\Gamma = 0 \tag{6}$$

For general metal, it is reported that good results can be achieved if the relative density of metal is set as 0.999[11]. The velocity field $\boldsymbol{u}$ and strain rate vector $\dot{\varepsilon}$ of the element can be approximately interpolated within an

element by the shape function $\boldsymbol{N}$ and nodal velocity vector $\boldsymbol{v}$ as follows:

$$\boldsymbol{u} = \boldsymbol{N}^{\mathrm{T}}\boldsymbol{v}, \quad \dot{\boldsymbol{\varepsilon}} = \boldsymbol{B}\boldsymbol{v} \tag{7}$$

The effective strain rate of P/M is defined as follows:

$$\left(\tilde{\dot{\varepsilon}}\right)^2 = \dot{\varepsilon}^{\mathrm{T}}\boldsymbol{D}\dot{\varepsilon} = \boldsymbol{v}^{\mathrm{T}}\boldsymbol{B}^{\mathrm{T}}\boldsymbol{D}\boldsymbol{B}\boldsymbol{v} = \boldsymbol{v}^{\mathrm{T}}\boldsymbol{P}\boldsymbol{v} \tag{8}$$

The matrix $\boldsymbol{P}$ can be decomposed with the shear deformation energy term $\boldsymbol{P_1}$ and the volumetric deformation energy term $\boldsymbol{P}_2$ while the material constant matrix $\boldsymbol{D}$ can be decomposed with $\boldsymbol{D_1}$ and $\boldsymbol{D_2}$ as follows :

$$\boldsymbol{P} = \boldsymbol{P_1} + \boldsymbol{P_2} = \boldsymbol{B}^{\mathrm{T}}\boldsymbol{D_1}\boldsymbol{B} + \boldsymbol{B}^{\mathrm{T}}\boldsymbol{D_2}\boldsymbol{B} \tag{9}$$

The functional of Eq. (6), then can be approximated in a finite dimensional space with finite elements as follows:

$$\sum_j \delta \boldsymbol{v}^{\mathrm{T}} \left[\sum_{e=1}^{E} \int_{\Omega_e} \frac{\tilde{\sigma}}{\tilde{\dot{\varepsilon}}} \boldsymbol{P_1}\boldsymbol{v}\, d\Omega + \sum_{e=1}^{E} \int_{\Omega_e} \frac{\tilde{\sigma}}{\tilde{\dot{\varepsilon}}} \boldsymbol{P_2}\boldsymbol{v}\, d\Omega - \sum_{e=1}^{E_1} \int_{\Gamma_{e,f}} \boldsymbol{N}\,\boldsymbol{f}\, d\Gamma \right]_j = 0 \tag{10}$$

And the potential energy of i-th component Φ_{i} is expressed as follows:

$$\Phi_i = \sum_{e=1}^{E} \int_{\Omega_e} \frac{\tilde{\sigma}}{\tilde{\dot{\varepsilon}}} P_{1ij} v_j\, d\Omega + \sum_{e=1}^{E} \int_{\Omega_e} \frac{\tilde{\sigma}}{\tilde{\dot{\varepsilon}}} P_{2ij} v_j\, d\Omega - \sum_{e=1}^{E_1} \int_{\Gamma_{e,f}} N_{ij} f_j\, d\Gamma = 0 \tag{11}$$

The velocity field that minimizes the potential energy can be acquired by the Newton-Raphson iteration method.

2.3 Formulations for arbitrary shaped die and contact treatment

An arbitrary shaped die can be described by a finite element patch method[12] with which the data storage is relatively small and treatment for the contact and a searching scheme is easy to deal with. Although triangular linear patch for the arc shaped die needs a lot of patches and special treatment for treating the curved part, it can describe complex geometry easily and carry out computation conveniently.

A contact problem can be treated by the penalty method or the Lagrange multiplier method [13]. In order to deal with the deformable body contact problem, the Lagrange multiplier method has been adopted for stable convergence, although unknowns and computation storage are larger than those with the penalty method. The skew boundary condition is used for the contact treatment between die and a material. The Lagrange multiplier method for contact between two bodies can be described as follows[13]:

$$\begin{bmatrix} \boldsymbol{K} & \boldsymbol{C}^T \\ \boldsymbol{C} & \boldsymbol{0} \end{bmatrix} \begin{Bmatrix} \boldsymbol{U} \\ \lambda \end{Bmatrix} = \begin{Bmatrix} \boldsymbol{R} \\ \boldsymbol{Q} \end{Bmatrix} \tag{12}$$

where $\boldsymbol{C}$ is the constraint vector, $\boldsymbol{\lambda}$ is the Lagrange multipliers and $\boldsymbol{Q}$ is the gap function.

In the contact problem of a deformable body, master segments and slave nodes take a role of die and contact nodes in the case of the rigid contact respectively. For the case of the master segment and slave nodes as shown in Fig. 1, a relation between the slave node and the master element can be expressed as:

$$\boldsymbol{F}(\mathrm{s,\,t},\lambda) = \boldsymbol{P}_{\mathrm{o}} - \boldsymbol{X}(s,t) - \lambda\,\boldsymbol{n} = \boldsymbol{0}, \quad \boldsymbol{X}(s,t) = \sum_{\alpha=1}^{4} N_{\alpha}(s,t)\boldsymbol{X}_{\alpha} \tag{13}$$

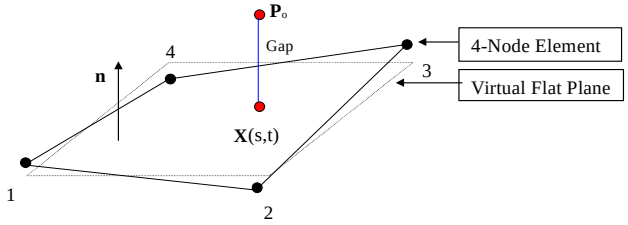

Fig.1 *Schematic relation between the slave node and master segment.*

where $\boldsymbol{n}$ is the normal vector of the virtual flat plane of the master element, N_α is the shape function and s and t are the local coordinate in an element. Fig. 2 shows the gap function between the master element and the slave node. The exact gap function ($g = \boldsymbol{Q}$) and the penetration position (s,t) can be obtained by applying the Newton-Raphson method after differentiating Eq. (13). The relation, then, can be expressed as $\{\boldsymbol{C}\}\{\boldsymbol{U}\}=\{\boldsymbol{Q}\}$ and the displacement and the gap function can be expressed as follows:

$$\boldsymbol{u}_m=\sum_{\boldsymbol{\alpha}=1}^{4} N_{\boldsymbol{\alpha}}(s,t)\boldsymbol{u}_{\boldsymbol{\alpha}}=\frac{1}{4}(1-s_m)(1-t_m)\boldsymbol{u}_1+\frac{1}{4}(1+s_m)(1-t_m)\boldsymbol{u}_2 + \frac{1}{4}(1+s_m)(1+t_m)\boldsymbol{u}_3+\frac{1}{4}(1-s_m)(1+t_m)\boldsymbol{u}_4 \tag{14}$$

$$g_s^i=\left(\boldsymbol{u}_m^{i+1}-\boldsymbol{u}_s^{i+1}\right)\cdot\boldsymbol{n}^i \tag{15}$$

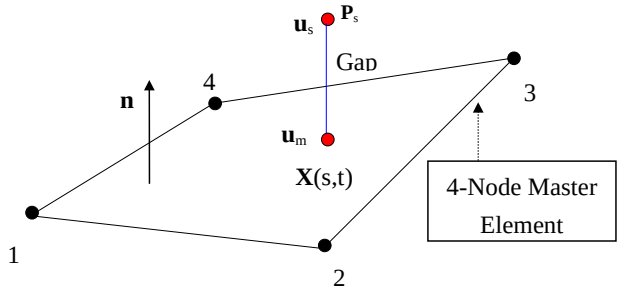

Fig.2 *Schematic relation between the gap and the displacement.*

$\boldsymbol{C}$ can be obtained with the use of Eq. (15) as follows:

$$\{\boldsymbol{C}\}=\{N_1n_x,\ N_1n_y,\ N_1n_z,N_2n_x,\ N_2n_y,\ N_2n_z,\ N_3n_x,\ N_3n_y,\ N_3n_z,N_4n_x,\ \ N_4n_z,\ -n_x,\ -n_y,\ -n_z\}_{1\times15} \tag{16}$$

And the corresponding $\{\boldsymbol{U}\}$ and $\{\boldsymbol{Q}\}$ can be expressed as follows:

$$\{\boldsymbol{U}\}^T=\{u_{1,x},\ u_{1,y},\ u_{1,z},\ u_{2,x},\ u_{2,y},\ u_{2,z},\ u_{3,x},\ u_{3,y},\ u_{3,z},\ u_{4,x},\ u_{4,y},\ u_{4,z},\ u_{s,x},\ u_{s,y},\ u_{s,z}\}_{1\times15} \tag{17}$$

$$\{\boldsymbol{Q}\}=\{g^i\} \tag{18}$$

The slave nodes, which contact die surface and the master element simultaneously, should be transformed in the skew coordinates. The global stiffness matrix and the global external force vector can be constructed by the transformation between the skew coordinates and the global coordinates.

3. Numerical results

3.1 Flat magnet model

A flat magnet model is analyzed to investigate the effectiveness of the code developed. The initial relative density of powdered magnet is 0.75, which is used in the real Tube Process (TP) and the relative density of a copper tube is fixed as 0.999 for a rigid-plastic material. The strain-stress relation of the two materials have been obtained by the experiment at the real TP temperature of 700 ^{o}C as follows[9]:

Copper Tube : $\bar{\sigma} = 17.24\bar{\varepsilon}^{0.12}$ (MPa) (19-a)

Nd-B-Fe Magnet : $\bar{\sigma} = 89.497\bar{\varepsilon}^{0.215}$ (MPa) (19-b)

A quarter model using 8-node hexahedral isoparametric elements is analyzed for the sake of geometric symmetry. Fig. 3 shows a finite element mesh model and die geometry for a flat magnet model.

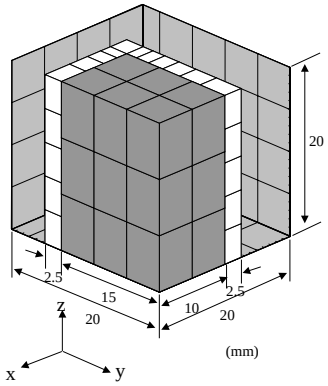

Fig. 3 *Initial F.E. mesh and die geometry for simple model*

Fig. 4 shows the deformed shapes with the variation of the height reduction. It can be seen that a tube separates from the magnet powder in the early stage of deformation. Both contact treatment between magnet and die and that between tube and magnet have been properly carried out.

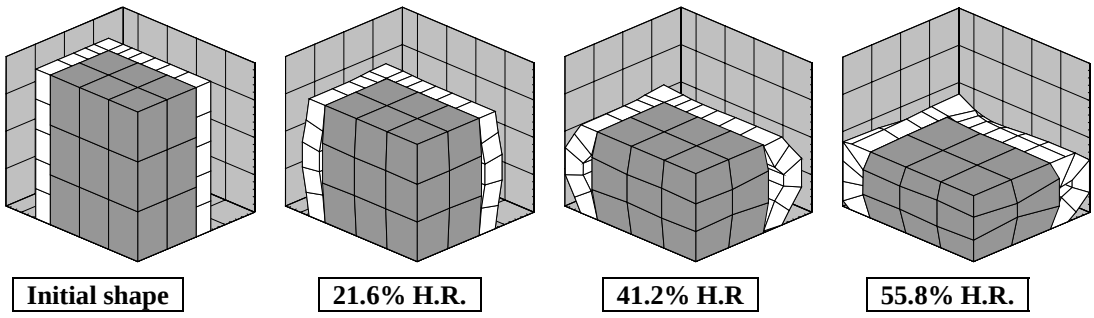

Fig. 4 *Initial and deformed shape for simple model*

3.2 Magnets for EHPS model – full Tube Process Simulation

Simulation of TP for EHPS magnet model is carried out with the same material properties as in the section 3.1. The magnet for EHPS are arc shaped with the upper die radius of 18.5 mm and the lower die radius of 21 mm. Fig. 5 describes a finite element mesh, dimensions and die geometry. Finite element patches of punch and dies are shown in Fig. 6. Slanted preform is adopted to reduce the folding of copper tube and obtain uniform densification[9].

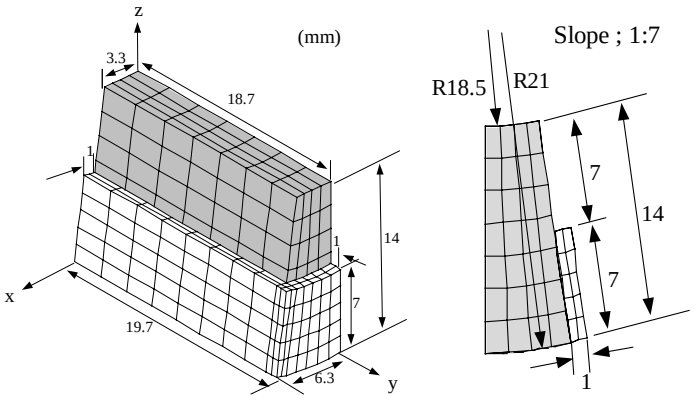

Fig. 5 *Finite element mesh , dimension of preform and geometry of the punch*

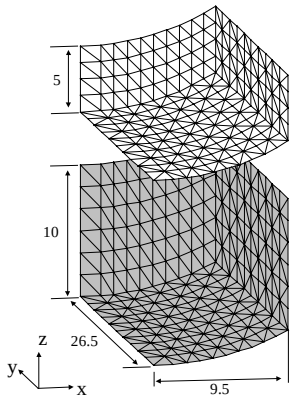

Fig. 6 *Finite element die patch EHPS magnet model*

Deformed shapes and relative density distributions with the variation to the height reduction are shown in Fig. 7. For the optimum process, a tube is located in the lower part of magnet powder. The relative density distribution becomes more uniform with the preform suggested than with others

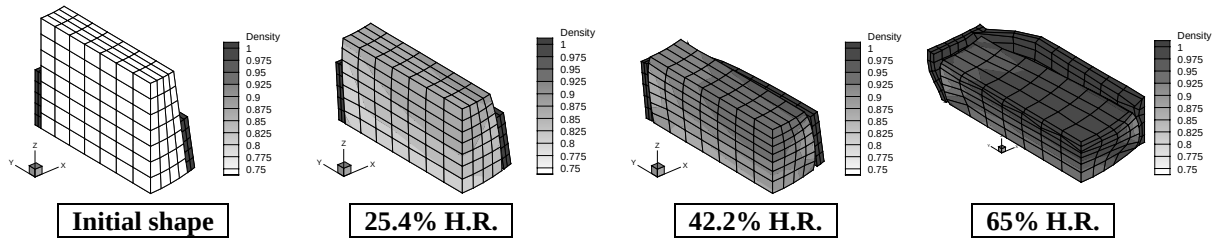

Fig. 7 *Initial and deformed shape with relative density distribution for EHPS magnet model*

4. Conclusion

The simulation has been carried out for a full TP in a closed die considering the compressibility of material, arbitrary curved shape and two contact types. TP for flat-type square magnet is simulated to verify the validity of the present code. TP for arc-shaped magnets for EHPS (Electro-Hydraulic Power Steering) system is simulated for the optimum preform design. In order to achieve net-shape manufacturing by reducing the flash and folding of the tube, the optimum preform of slanted shape is selected with the proper initial dimension. Results show that the finite element analysis of TP is indispensable in the stage of the preform design.

References

1) Green, R. J. (1972) A Plasticity Theory for Porous Solids. *Int. J. Mech. Sci*. 14, pp. 215-224.
2) Shima, S. and Oyane, M. (1976) Plasticity Theory for Porous Metals. *Int. J. Mech. Sci*. 18, pp. 185-191.
3) Doraivelu, S. M., Gegel, H. L., Gunasekera, J. S., Malas, J. C., Morgan, J. T. and Thomas, Jr., J. F. (1984) A New Yield Function for Compressible P/M Materials. *Int. J. Mech. Sci*. 26, pp. 527-535.
4) Seetharaman, V., Doraivelu, S. M. and Gegel, H. L. (1990) Plastic Deformation Behavior of Compressible Solids. *J. Mater. Shaping Technol.* 8, pp. 239-248.
5) Kuhn, H. A. and Downey, C. L. (1973) Material Behavior in Powder Preform Forging. *Trans. ASME, J. of Eng. Mater. Technol.* 95, pp. 41-46.
6) Mori, K. (1982) Finite Element Method of Rigid-Plastic Analysis of Metal Forming. *Int. J. Mech. Sci*. 24, pp. 459-465.
7) Chenot, J. L., Bay, F. and Fourment, L. (1990) Finite Element Simulation of Metal Powder Forming. *Int. J. Numer. Methods Eng.* 30, pp. 1649-1674.
8) Zienkiewicz, O. C., Huang, G. C. and Liu, Y. C. (1990) Adaptive FEM Computation of Forming Process – Application to Porous and Non-Porous Materials. *Int. J. Numer. Methods Eng.* 30, pp. 1527-1553.
9) Kim, S. H., Lee, C. H. and Huh, H. (1999) Preform Design for the Sinter-forging Process of Arc-shaped Powdered Magnets. *Trans. of Materials Processing.* 8, pp. 135-142.
10) Kobayashi, S., Oh, S.I. and Altan, T. (1989) *Metal forming and the finite element method.* Oxford University Press.
11) Mori, K., Shima, S. and Osakada, K. (1980) FEM for the Analysis of Plastic Deformation of Porous Metals. *Bulletin of the JSME*. 23, pp. 516-522
12) Schweizerhof, K. & Hallquist, J. Q. (1991) Explicit Integration Schemes and Contact Formulations for thin sheet forming. *Proc. Verein Deutscher Ingenieure* (ed. by T. Altan *et al.*), Zurich, Swizerland, pp. 405-439.
13) Zhong, Z.H. (1993) *Finite Element Procedures for Contact-Impact Problems.* Oxford Univ. Press.